Preparation of Cu₂O Superhydrophobic Film with Hierarchical Structure *via* the Facile Route

MINGDE PEI[1], BO WANG[1,*], YUNHUI TANG[1], XUEHONG ZHANG[1], HUI YAN[1] and XIAOXUE ZHANG[2]

[1]Department of Materials Science and Engineering, Beijing University of Technology, Beijing 100124, P.R. China
[2]Laboratory of Ceramic Materials, Department of Materials Science, Tampere University of Technology, P.O.Box 589, FI-33101 Tampere, Finland

*Corresponding author: Tel: +86 10 67396274; E-mail: wangbo@bjut.edu.cn

A Cu₂O layer was employed as a new method to achieve the superhydrophobicity on a copper surface using a simple hydrothermal method. First, a Cu₂O layer with a hierarchical structure was grown on the copper surface using an oxidization step and it exhibited the hydrophilicity. The analysis results of XRD and XPS confirmed the formation of a Cu₂O phase on the copper surface. Second, the Cu₂O surface was changed to superhydrophobicity *via* a modifying process using $1H,1H,2H,2H$-perfluorodecyltriethoxysilane. Peaks corresponding to F1s, -CH₂, -CF₂ and -CF₃ groups in the XPS spectra confirm the assemblage of the F-contained radicals on the surface. The wetting mechanism is discussed briefly. Wetting tests also demonstrate that a water droplet on the surface can slide away very easily, even with only a slight tilt and that it has a lower adhesion to the modified surface.

Keywords: Surface oxidation, Superhydrophobic surface, Hierarchical structure, Contact angle.

INTRODUCTION

Water-repellent surfaces with a water contact angle higher than 150º are known as superhydrophobic surfaces. A water droplet on a superhydrophobic surface will roll off at a small tilt angle. After the discovery of the important role of the hierarchical structure of superdydrophobic surfaces in nature (*e.g.* the lotus leaves), many artificial superhydrophobic coatings have been developed to mimic the lotus leaves. In order to achieve such a bionic superhydrophobic surfaces, both the low surface energy and the rough morphology are necessary[1]. Many techniques, such as assembling, electrochemical deposition, sol-gel, *etc.*, have been used to prepare such surfaces[2-7]. However, these methods are still complicated and or expensive. For practical applications, further efforts are needed to find more convenient and economical techniques.

Copper is an important common material and has been widely used in many fields. The surface wettability of copper has been extensively studied[8,9]. A contact angle of 161º has been achieved on a flower-like CuO superhydrophobic surface by Chen *et al.*[10]. The above mentioned studies on surface wettability are mainly concerned with the surfaces of Cu, CuO, or Cu(OH)₂[11,12]. Here Cu₂O is employed in a different way, Cu₂O is usually thought of a typical *p*-type direct band gap semiconductor with a band gap of 2.17 eV and has potential applications in solar energy conversion[13], electrode materials,

sensors and catalysts[14,15]. Various interesting cuprous oxide nanostructures such as cubes, cuboctahedra, octahedra, multipods, nanowires and hollow structures have been synthesized by wet chemical reduction[16-19], electrodeposition[20-22] and solvothermal synthesis methods[23-25]. While most of the studies focus on powders largely more than films. Moreover, the wettability of Cu₂O film has been less studied.

In the present work, Cu₂O film was synthesized using a facile hydrothermal method to form the necessary hierarchical structure necessary for a superhydrophobic surface. The prepared surface exhibits an excellent superhydrophobic property with a contact angle of 159º. The water droplet can easily slide on the surface, even with a slight tilt angle and compared to an unmodified surface, has a lower adhesion to the modified surface.

EXPERIMENTAL

All the reagents were commercially available with analytical grade and used without further purification. First, a copper plate with a size of 2 cm × 2 cm × 0.01 cm (purity 99.9 %, purchased from Chemical Reagent ,Tianjin) is etched in 2 M HCl for 30 s to remove surface oxides and then ultrasonically cleaned in ethanol and deionized water for 15 min, respectively. Following the clean is an oxidation step that includes immersing the sample into a 0.02 M aqueous solution of sodium dodecyl-benzenesulfonate (DDBS) and then transferring the solution into a Teflon-lined stainless steel autoclave

of 50 mL capacity, sealed and maintained at 200 ºC for 12-48 h. When the steel autoclave has cooled down to room temperature and the immersed copper plate is rinsed with deionized water and ethanol thoroughly and then dried in air. Next, the oxidized copper plate is immersed in an ethanol solution of 1*H*,1*H*,2*H*,2*H*-perfluorodecyltriethoxysilane (PDES) (alfa aesar purity 97 %) for 1 h. Finally, after being rinsed in ethanol, the sample is heated at 120 ºC for 1 h at low pressure (1 Pa) to finish preparing the samples. The samples were analyzed using an X-ray diffractometer of D8 advance with CuK$_{\alpha 1}$ radiation (λ = 1.5405 Å). The morphologies of the samples were observed using an S-3400N scanning electron microscope (SEM). Contact angles (CA) of water drops on the surface were measured using a GonioStar150 CA measurement instrument. Analysis of the chemical elements present on the copper surface was carried out using an ESCALab250 X-ray photoelectron spectrometer (XPS).

RESULTS AND DISCUSSION

Fig. 1 shows the surface scanning electron microscopy (SEM) images of the original copper plate and of the oxidized surface. It is clear that many large crystal grains several microns in size exist on the oxidized surface and that smaller grains in the hundreds of nanometers range have grown under the large grains, composing a kind of hierarchical structure.
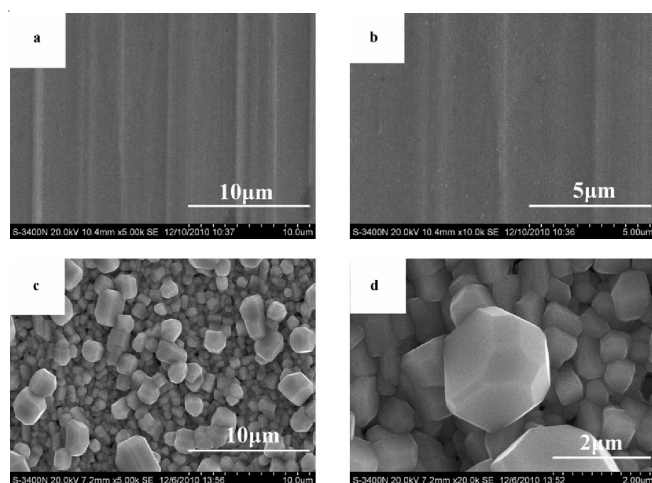

Fig. 1.   (a) and (b) are the SEM images of the original copper surface with the magnifications of 5 and 10 K, respectively and (c), (d) are those of the oxidized surface

Fig. 2 shows the XRD patterns from the copper plate and the as-prepared surface. In the pattern from the original copper surface, there are three peaks corresponding to the diffraction lines of cubic copper in the (111), (200) and (220) orientations, respectively. These suggests that the copper plate contains solely a cubic copper phase. In the pattern from the oxidized surface, four additional peaks appear. These reveal the existence of a Cu$_2$O phase on the surface according to the standard card of PDF#05-0667. The four additional peaks correspond to the diffraction lines of Cu$_2$O in the (110), (111), (200) and (220) orientations, respectively. The process of forming the crystal morphology of the Cu$_2$O has been reported earlier[16-19]. For the cubic phase, the surface energy value, $\gamma\{111\} < \gamma\{100\} < \gamma\{110\}$, can be easily deduced from the
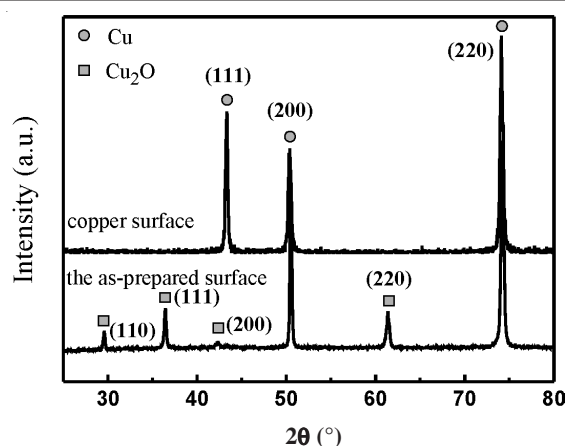

Fig. 2.   XRD patterns of the copper surface and the oxidized surface, respectively

distances between these three crystal planes and the central Wulff's point. From a crystallographic point of view, Cu$_2$O is a cuprites structure and the amount of the Cu^{1+} is twice that of the O^{2-} tetrahedral. The structure can be described as a cubic close packing of copper atoms. The {111} and {100} planes in the Cu$_2$O crystal lattice are different in the surface atom structures. The surface with plane {111} is nonpolar, whereas with plane {100} is polar. According to Gibbs-Wulff's theory, both the {111} and {100} planes are often remained in the final appearance. Generally, the growth of dipolar Cu$_2$O crystal dependent on not only their polar characteristic, but also the supersaturation of the solute. Under equilibrium condition, the inorganic crystal growth are determined by the relative order of surface energies. The fastest crystal growth will occur on the surface with the highest surface energy. This results in the elimination of higher-energy surfaces while the lower-energy surfaces increase in area. When the dodecyl benzene sulfonate are added during the crystal growth process, the relative order of surface energies can be changed. Because of the anisotropy adsorbability, these additives adsorb onto a certain crystallographic plane more strongly than others. This preferential adsorption lowers the surface energy of the bound plane and hinders the crystal growth on it, resulting in a change in the final morphology of Cu$_2$O[26,29].

The surface of the hierarchical structure of Cu$_2$O was chemically modified with PDES to improve the hydrophobicity. Fig. 3(a) shows the typical XPS spectra of the Cu$_2$O hierarchical structure both before and after chemical modification with 1*H*,1*H*,2*H*,2*H*-perfluorodecyltriethoxysilane (PDES). The peaks corresponding to Si2p, C1s and F1s in the spectra of the chemically modified sample reveal that the radicals containing fluorine had been successfully assembled onto the surface of the hierarchical structure. Fig. 3(b) shows the high resolution XPS spectrum of the sample modified using 1*H*,1*H*,2*H*,2*H*-perfluorodecyltriethoxysilane. The peaks at 284.8, 291.4 and 293.6 eV can be assigned to the -CH$_2$, -CF$_2$ and -CF$_3$ groups, respectively[10], which also confirms the assemblage of the F-contained radicals onto the surface as well. In Fig. 3(c), the Cu2p$_{1/2}$ and Cu2p$_{3/2}$ peaks also confirm the existence of the Cu$_2$O phase[30-32], this agrees well with the XRD results.

Just as with most metals, the original copper surface is hydrophilic with a contact angle of 69º. Fig. 4(a-c) showed the
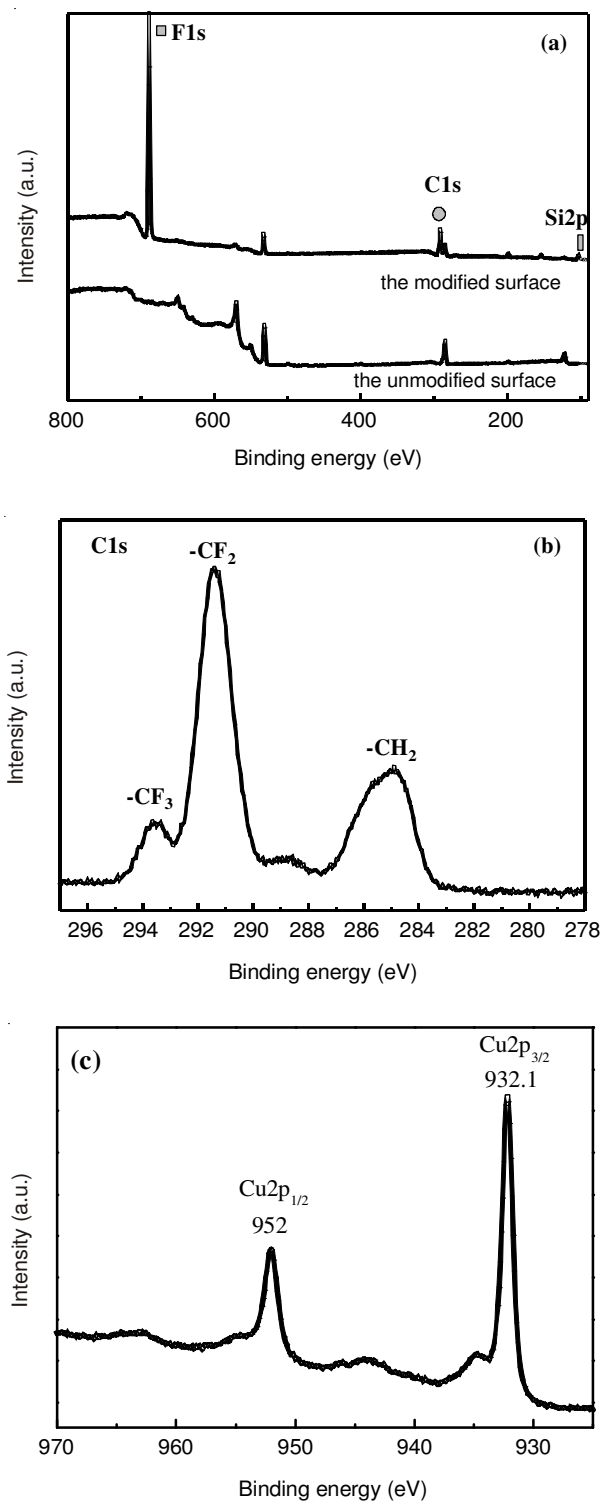
Fig. 3. XPS data of (a) the spectrum of the unmodified surface and the modified surface with PDES, (b) C1s spectrum of the modified surface, (c) Cu2p spectrum of the modified surface

contact angle images of the oxidized surface before and after being modified using PDES. After being oxidized in a reaction solution at 200 °C, the surface morphology and chemical properties have been changed and the surface contact angle has been reduced to 14° (Fig. 4(b)). In addition to the influence on the chemical properties, the reduction of the contact angle may also be explained by the Wenzel theory: for a hydrophilic surface, surface roughness contributes to the improvement of wettability.
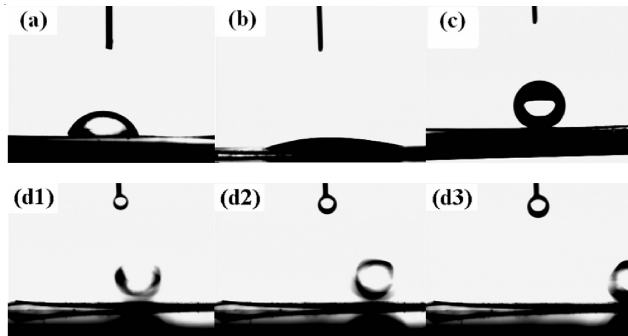

Fig. 4. (a) a water droplet on the original copper surface; (b) a water droplet on the oxidized surface before and (c) after modified with PDES; (d) the water droplet sliding photos on the PDES-modified surface taken with a interval of 60 ms (d1 to d3)

After being treated with PDES, the contact angle of the oxidized surface has changed from 14 to 159° [Fig. 4(c)] and is dominated mainly by a reduction in the surface free energy of the rough surface.

When the surface modified with PDES is tilted slightly, the water droplet on it can easily slide. Fig. 4(d) shows photos of a water droplet sliding at the superhydrophobic surface. The adhesion of a water droplet to the modified surfaces was also tested using the method reported by Gao *et al.*[33]. Fig. 5 shows the contact, deformation and departure processes of a water droplet suspended from a syringe contacting a modified surface. The water droplet can easily and completely leave from the modified surface.
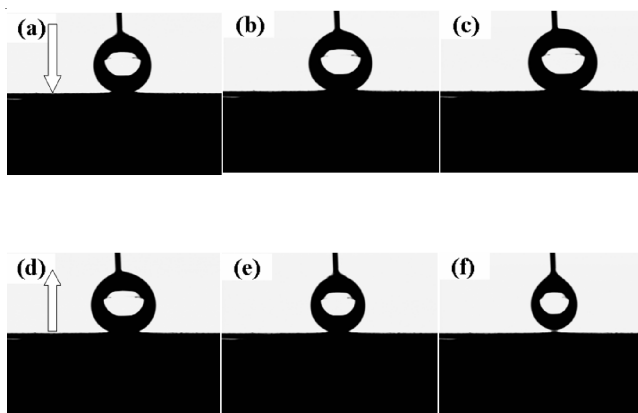

Fig. 5. Contact, deformation and departure processes of water droplet suspending on a syringe with the modified surface. the arrows represent the moving direction of the water droplet

To understand the superhydrophobicity of a hierarchical surface fully, the Cassie and Baxter equation can be used:

$$\cos\theta_r = f_1 \cos\theta - f_2$$

where θ_r and θ represent for the contact angles of the rough and smooth surface, respectively; and f_1 and f_2 are the fractions of the interface area of solid-water and air-water, respectively. According to the Cassie-Baxter equation, the increasing fraction of air-water surface leads to an increase in the contact angle on a rough surface. In this paper, θ_r and θ (118° in our practical test) are the contact angles of the final sample surface and of a PDES-modified smooth copper surface, respectively. In the present studies, the f_2 value of the PDES-modified surface is estimated to be 0.88, which indicates that a large fraction of

air is trapped in the hierarchical structures after they have been created by chemically modified. This has led to the superhydrophobicity of the surface.

Conclusion

High hydrophilic and superhydrophobic Cu_2O surfaces have been created using different solution modification methods. Through an oxidization process, a Cu_2O layer with a kind of hierarchical morphology was grown on the copper surface and the contact angle of the surface was reduced to 14º from the original value of 69º. Modified using PDES in the subsequent step, the surface was changed to be super hydrophobic with a contact angle of 159º and a low sliding angle less than 5º. The analysis of XPS spectra of the PDES-modified sample reveals that the F-contained radicals have been successfully assembled onto the surface. According to the Cassie-Baxter equation, the fraction of contact area between solid and water, f_2, was estimated to be 0.88. Both the surface morphology and the F-contained radicals are considered to be the determinants of the superhydrophobicity and low sliding angle. Moreover, the surface shows a low adhesion for water and a long-term stability.

REFERENCES

1. T.L. Sun, L. Feng, X.F. Gao and L. Jiang, *Acc. Chem. Res.*, **38**, 644 (2005).
2. J.D. Wang, A. Li, H.S. Chen and D.R. Chen, *J. Bionic Eng.*, **8**, 122 (2011).
3. X.X. Zhang, M. Honkanen, M. Järn, J. Peltonen, V. Pore, E. Levänen and T. Mäntylä, *Appl. Surf. Sci.*, **254**, 5129 (2008).
4. X.Y. Ling, I.Y. Phang, G.J. Vancso, J. Huskens and D.N. Reinhoudt, *Langmuir*, **25**, 3260 (2009).
5. Y. Zhao, S.J. Xie and Y.J. Jiang, *Surf. Interface Anal.*, **44**, 1360 (2012).
6. Z.G. Guo, W.M. Liu and B.L. Su, *Appl. Phys. Lett.*, **92**, 063104 (2008).
7. G.L. Song, S.D. Ma, G.Y. Tang and X.W. Wang, *Colloid. Surf. A*, **364**, 99 (2010).
8. N.J. Shirtcliffe, G. McHale, M.I. Newton, G. Chabrol and C.C. Perry, *Adv. Mater.*, **16**, 1929 (2004).
9. J.M. Xi, L. Feng and L. Jiang, *Appl. Phys. Lett.*, **92**, 053102 (2008).
10. X.H. Chen, L.H. Kong, D. Dong, G.B. Yang, L.G. Yu, J.M. Chen and P.Y. Zhang, *J. Phys. Chem. C*, **113**, 5396 (2009).
11. Z.G. Guo, W.M. Liu and B.L. Su, *Appl. Phys. Lett.*, **92**, 063104 (2008).
12. Q.M. Pan, M. Wang and H.B. Wang, *Appl. Surf. Sci.*, **254**, 6002 (2008).
13. A.O. Musa, T. Akomolafe and M.J. Carter, *Sol. Energ. Mater. Sol. Cells*, **51**, 305 (1998).
14. X. Li, H. Gao, C.J. Murphy and L. Gou, *Nano. Lett.*, **4**, 1903 (2004).
15. J.T. Zhang, J.F. Liu, Q. Peng, X. Wang and Y.D. Li, *Chem. Mater.*, **18**, 867 (2006).
16. L.F. Gou and C.J. Murphy, *Nano. Lett.*, **3**, 231 (2003).
17. M.H. Kim, B. Lim, E.P. Lee and Y. Xia, *J. Mater. Chem.*, **18**, 4069 (2008).
18. X.D. Liang, L. Gao, S.W. Yang and J. Sun, *Adv. Mater.*, **21**, 2068 (2009).
19. L.S. Xu, X.H. Chen, Y.R. Wu, C.S. Chen, W.H. Li, W.Y. Pan and Y. Wang, *Nanotechnology*, **17**, 1501 (2006).
20. S. Sahoo, S. Husale, B. Colwill, T.M. Lu, S. Nayak and P.M. Ajayan, *ACS Nano*, **3**, 3935 (2009).
21. E.W. Bohannan, M.G. Shumsky and J.A. Switzer, *Chem. Mater.*, **11**, 2289 (1999).
22. A.D. Tang, Y. Xiao, J. Ouyang and S. Nie, *J. Alloys Compd.*, **457**, 447 (2008).
23. H.W. Zhang, X. Zhang, H.Y. Li, Z.K. Qu, S. Fan and M.Y. Ji, *Cryst. Growth Des.*, **7**, 820 (2007).
24. H.G. Zhang, Q.S. Zhu, Y. Wang, C.Y. Zhang and L. Tao, *Mater. Lett.*, **61**, 4508 (2007).
25. Y.Y. Xu, X.L. Jiao and D.R. Chen, *J. Phys. Chem. C*, **112**, 16769 (2008).
26. Y.M. Sui, W.Y. Fu, H.B. Yang, Y. Zeng, Y.Y. Zhang, Q. Zhao, Y.G. Li, X.M. Zhou, Y. Leng, M.H. Li and G.T. Zou, *Cryst. Growth Des.*, **10**, 99 (2010).
27. D.F. Zhang, H. Zhang, L. Guo, K. Zheng, X.D. Han and Z. Zhang, *J. Mater. Chem.*, **19**, 5220 (2009).
28. C.-H. Kuo and M.H. Huang, *Nano Today*, **5**, 106 (2010).
29. M.J. Siegfried and K.-S. Choi, *Adv. Mater.*, **16**, 1743 (2004).
30. K.H. Yoon, W.J. Choi and D.H. Kang, *Thin Solid Films*, **372**, 250 (2000).
31. W.Z. Wang, G.H. Wang, X.S. Wang, Y.J. Zhan, Y.K. Liu and C.L. Zheng, *Adv. Mater.*, **14**, 67 (2002).
32. J.J. Teo, Y. Chang and H.C. Zeng, *Langmuir*, **22**, 7369 (2006).
33. X.F. Gao, X. Yao and L. Jiang, *Langmuir*, **23**, 4886 (2007).